

## Al-Doped Mesoporous Cellular Foam Modified Electrode as Sensor for the Detection of Parathion Pesticide

Liang Wei<sup>1</sup>, Xinlong Huang<sup>1</sup>, Feiyan Yan<sup>2</sup>, Lufei Zheng<sup>3</sup>, Jing Wang<sup>3</sup>, Liping Xie<sup>2</sup>, Yu Ya<sup>2,\*</sup>

<sup>1</sup> College of Chemistry and Materials Science, Guangxi Teachers Education University, Nanning 530001, China

<sup>2</sup> Institute for Agricultural Product Quality Safety and Testing Technology, Guangxi Academy of Agricultural Sciences, Nanning 530007, China

<sup>3</sup> Institute of Quality Standard & Testing Technology for Agro-Product, Chinese Academy of Agricultural Sciences, Beijing 100081, China

\*E-mail: [yayu1026@163.com](mailto:yayu1026@163.com)

Received: 3 October 2018 / Accepted: 5 November 2018 / Published: 5 January 2019

---

Al-doped mesoporous cellular foam (Al-MCF) materials have been synthesized using “pH-adjusting” method and characterized by transmission electron microscopy (TEM), scanning electron microscopy coupled with energy dispersive X-ray spectrometry (SEM-EDS), X-ray diffraction (XRD), and nitrogen physisorption. The prepared Al-MCF was used to construct a carbon paste electrode (Al-MCF/CPE) for the electroanalysis of ethyl parathion (EP). Electrochemical behaviors of EP at the bare carbon paste electrode (CPE) and Al-MCF/CPE were studied. The results showed that the voltammetric response of EP at the Al-MCF/CPE sharply increased due to the high adsorption capacity, large surface area, and excellent electron transport properties of the Al-MCF. Some parameters, such as the content of Al-MCF, accumulation time, accumulation potential, and pH were optimized. Under optimal conditions, the oxidation peak current was proportional to EP concentration in the ranges of 0.010 to 0.10 mg/L and 0.10 to 1.0 mg/L, respectively, with a detection limit of 0.0050 mg/L (S/N = 3). The proposed method was applied for the determination of EP in vegetable samples with the recoveries of 94.4 – 110 %.

---

**Keywords:** Al-doped mesoporous cellular foam, Modified electrode, Ethyl parathion, Electroanalysis

### 1. INTRODUCTION

Ethyl parathion (O,O-diethyl O-*p*-nitrophenyl phosphorothioate, EP) is a typical member of the organophosphorous pesticide family, which is widely used to control diseases of fruits and vegetables. However, concerns are being raised due to the high toxicity induced to living beings [1]. It can produce

serious hazards to human health even when it is found in traces. Hence, it is important to provide sensitive and accurate analytical methods for determination of EP. Several analytical techniques were used to determine the EP, such as chromatography [2-4], spectrophotometry [5], capillary electrophoresis [6], enzyme-linked immunosorbent assay [7], and electrochemistry [8-13]. Among all these approaches, the electroanalytical methods are preferred for the detection of EP due to the particular advantages, such as high sensitivity, ease of operation, short analysis time, and low cost. Recently, nanomaterials have been used as novel modifiers to construct various EP electrochemical sensors. For example, Sanghavi and co-workers proposed an EP electrochemical sensor based on carbon nanoparticles and halloysite nanoclay modified electrode [11], Bui and Seo developed a sensitive electroanalysis method for EP detection based on zirconium oxide–laponite nanocomposites modified electrode [12], Lima et al. reported a fast and facile strategy for the detection of EP by using a silver nanoparticles modified electrode [13]. All these nanomaterials based electrodes are considered as an efficient strategy for EP detection due to the advantages brought by the nanoparticles included in these electrodes, such as high surface area-to-volume ratio, high activity, and excellent electron transport properties.

Recently, the mesoporous cellular foam materials were described as ideal candidates for electrochemical sensors due to their unique three-dimensional mesoporous structure [14-16]. Moreover, the doping of these mesoporous cellular foam materials with metals has become an attractive topic, because the metal introduced into the framework not only maintains the original structure of mesoporous cellular foam materials, but also provides the material with catalytic activity [17].

In this work, Al-doped mesoporous cellular foam (Al-MCF) materials have been synthesized using the “pH-adjusting” method. The experimental results showed that the aluminum species can be doped into the wall of mesoporous cellular foam materials while maintaining the foam-like mesostructure. An EP electrochemical sensor based on Al-MCF was fabricated. The prepared sensor has the advantages of easy construction and high sensitivity. Moreover, the sensor exhibited significantly improved electrochemical oxidation of EP alongside with a high adsorption capacity, large electrode surface, and excellent electron transport properties.

## **2. EXPERIMENTAL**

### *2.1. Reagents and Instruments*

EP (99%) was obtained from Dr. Ehrenstorfer GmbH (Augsburg, Germany). P123 ( $\text{EO}_{20}\text{PO}_{70}\text{EO}_{20}$ , average molecular weight 5800) surfactant was obtained from Sigma Chemical Co. (St. Louis MO, USA). Graphite powder (spectral reagent) and paraffin oil were purchased from Sinopharm Chemical Reagent Co., Ltd (Shanghai, China). All other reagents were of analytical grade and were used as received. A phosphate buffer solution (PBS) was prepared from KOH and 0.1 M  $\text{H}_3\text{PO}_4$ , and the pH was monitored using a pH meter. All aqueous solutions were prepared in deionized water.

Transmission electron microscopy (TEM) images were obtained using a Tecnai G<sup>2</sup> F20 S-Twin microscope (FEI Ltd., USA). Scanning electron microscopy coupled with energy dispersive X-ray

spectrometry (SEM-EDS) images were taken on a SU8010 field-emission scanning electron microscope (Hitachi, Japan) equipped with an energy-dispersive detector (EDS) for the determination of elemental composition of the sample. X-ray diffraction (XRD) measurements were carried out with a Bruker Advanced D8 diffraction instrument using Cu  $K\alpha$  radiation (Karlsruhe, Germany). Nitrogen absorption-desorption isotherms were measured using an Autosorb-1-C-TCD-MS instrument (Florida, USA). All the electrochemical measurements were conducted using a CHI660D electrochemical workstation (Shanghai, China). A conventional three-electrode system was used for all electrochemical experiments with a bare or modified CPE ( $d = 3.0$  mm) as the working electrode, a platinum wire as a auxiliary electrode and a saturated calomel electrode (SCE) as a reference electrode. The pH of PBS was measured using a Leici pH-2 pH meter (Shanghai, China).

## 2.2. Synthesis of Al-MCF

Al-MCFs were synthesized by “pH-adjusting” method [18], and the procedures Accordingly, 10.0 g of P123 and 350 mL of 2M HCl solution were mixed at 35 °C, then 16.0 g benzene was added to the solution. After the solution was stirred for 1 h, 0.41 g of aluminium isopropoxide was added and the stirring was allowed for 2 h. Subsequently, 21.0 g of tetraethylorthosilicate was gradually added, and the solution was stirred at 35 °C for 24 h. The obtained mixture was then placed in a Teflon bottle and kept at 100 °C for 24 h. After that, ammonia was added dropwise into the solution to adjust the pH to 7.5. Then, the mixture was hydrothermally treated at 100 °C for another 24 h. The solids were collected and washed with 5000 mL deionized water. Finally, the samples were dried at 100 °C for 24 h and calcined at 550 °C for 5 h in air.

## 2.3. Preparation of modified electrode

The modified electrodes were prepared by thoroughly mixing 0.0250 g of Al-MCF with 1.00 g of the graphite powder and 0.5 mL of paraffin oil. The mixing was maintained until a homogenous wetted paste was obtained. The resulting paste was firmly packed into the cavity (3.0 mm diameter) of a polytetrafluoroethylene tube fitted with a copper piston, which serves as an inner electrical contact. Finally, the surface was polished on a smooth paper for later use. In the absence of Al-MCF, the bare CPE was prepared using the same procedure.

## 2.4. Electrochemical Measurement

The electrochemical measurements were conducted in a conventional electrochemical cell containing 10 mL of PBS (pH = 7.0), which contained a certain amount of EP. After accumulation for 240 s under -0.40 v, the square wave voltammetry (SWV) measurements were recorded from -0.60 to 0.50 V. The peak currents at about -0.14 v were measured for EP oxidation with a frequency of 15 Hz, an amplitude of 25 mV, and a step potential of 4 mV.

### 2.5. Sample preparation

The cabbage sample (10 g) was cleaned, homogenized and then subjected to extraction with 50 ml of diethyl ether. The obtained liquids were filtered through a 0.22  $\mu\text{m}$  membrane and then evaporated to dryness. Finally, the residues were redispersed in 5.0 mL of ethanol and diluted to 10 mL with PBS (pH = 7.0).

## 3. RESULTS AND DISCUSSION

### 3.1. Characterization of Al-MCF

The morphology of Al-MCF was analyzed by transmission electron microscopy. A representative TEM image is displayed in Figure 1A. The image clearly shows that the Al-MCF with three-dimensional mesoporous structure has been successfully prepared. Such a structure is highly beneficial for maintaining high surface area on the modified electrode and the diffusion of analytes [19,20]. The SEM-EDS elemental mapping was used to evaluate the distribution of Al species in the sample. As Figure 1B shows, the Al atoms (green color) were uniformly distributed within the Al-MCF framework. It is worth mentioning that, as shown previously, the high distribution of Al species is beneficial to maintain the mesoporous organization of the resulted MCF.

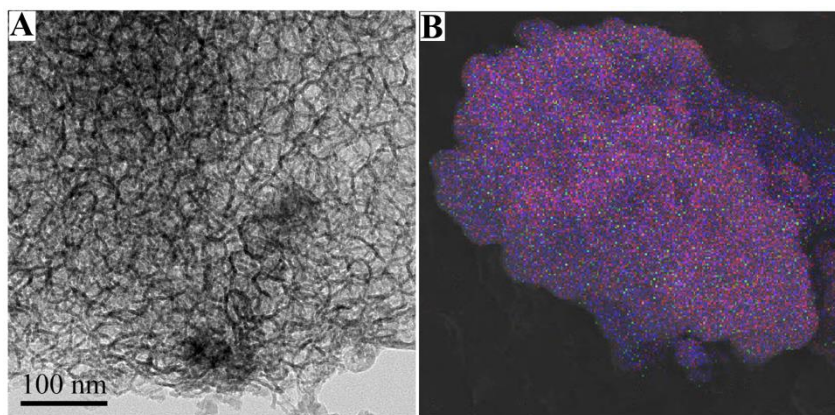


**Figure 1.** TEM image of Al-MCF (A). SEM-EDS mapping of Al-MCF, green colors represent Al element, blue colors represent Si element, and red colors represent O element (B).

The Al-MCF structure was further investigated by XRD. Figure 2A shows the XRD pattern in the  $2\theta$  range of  $10\text{--}80^\circ$  for the prepared Al-MCF. A broad diffraction peak can be observed between  $10$  and  $40^\circ$  with a maximum at  $\sim 25^\circ$ , which is the typical diffraction peak of amorphous silica. To note, no diffraction peaks are identified at high  $2\theta$  angle indicating that no crystalline Al species were formed. Moreover, the absence of these peaks clearly suggests the high distribution of the aluminum species obtained by “pH-adjusting” approach [21]. The nitrogen adsorption–desorption isotherm of the Al-MCF is shown in Figure 2B. The isotherm is of type IV with a hysteresis of type H1, according to IUPAC

classification, specific to mesoporous materials [22]. The pores size distribution curves (Figure 2C) contains each a maximum at 6.8 and 21.5 nm, respectively, which correspond to the windows and cells type pores developed in MCF silica. The surface area and the pore volume of Al-MCF were calculated based on the recorded isotherm and applying specific equations. For instance, the Brunauer–Emmett–Teller (BET) method was used to assess the surface area while the pore volume was calculated at a relative pressure,  $p/p_0$ , close to 1. Hence, a BET surface area and a total pore volume of  $417 \text{ m}^2\text{g}^{-1}$  and  $2.44 \text{ cm}^3\text{g}^{-1}$ , respectively, were obtained for the prepared Al-MCF.

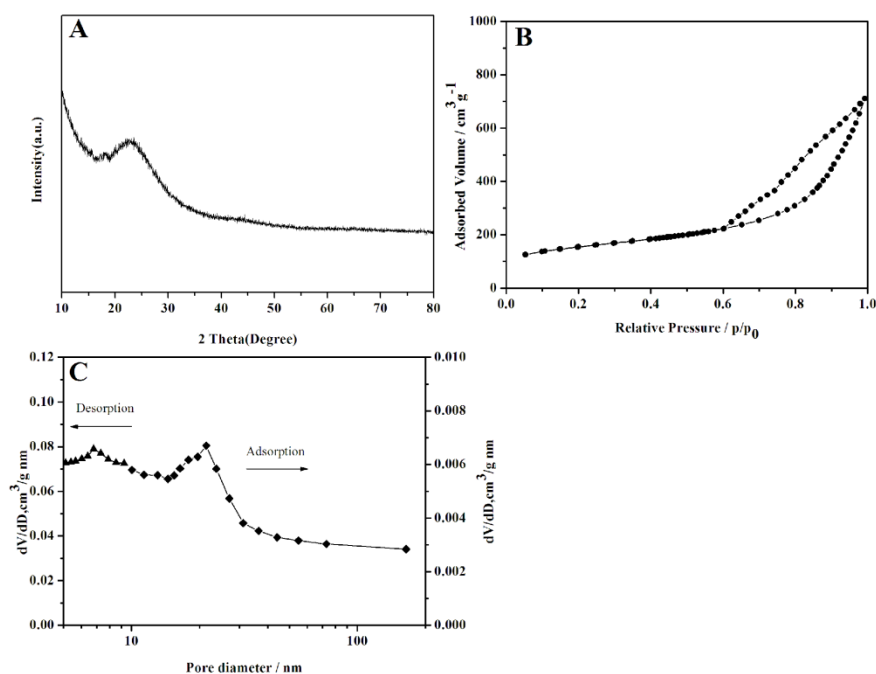


**Figure 2.** XRD pattern (A), nitrogen adsorption–desorption isotherm (B) and pore size distribution curve (C) of Al-MCF

### 3.2. Characterization of electrode

$[\text{Fe}(\text{CN})_6]^{3-/4-}$  was employed as a probe to investigate the electrochemical properties of the different electrodes. Figure 3A shows the cyclic voltammograms obtained for the bare CPE (curve a) and Al-MCF modified CPE (Al-MCF/CPE, curve b) in 5.0 mM  $[\text{Fe}(\text{CN})_6]^{3-/4-}$  solution. It can be observed that, in comparison with the bare CPE, a notable increased of peak current characterizes the curve obtained for Al-MCF/CPE. In the presence of  $[\text{Fe}(\text{CN})_6]^{3-/4-}$ , the peak-to-peak separation is 200 mV for the bare CPE while it decreases to 106 mV for the Al-MCF/CPE. These indicate that Al-MCF enhances the conductivity and electron transfer process. The electroactive area,  $A$ , was calculated from the Randles–Sevcik equation provided below [23].

$$I_p = 2.69 \times 10^5 D^{1/2} n^{3/2} A \nu^{1/2} C \quad (1)$$

where  $I_p$  refers to the peak current ( $\mu\text{A}$ ),  $D$  is the diffusion coefficient ( $\text{cm}^2 \text{s}^{-1}$ ),  $n$  is the electron-transfer number,  $A$  is the electroactive surface area of the electrode ( $\text{cm}^2$ ),  $\nu$  is the scan rate ( $\text{V s}^{-1}$ ), and  $C$  is the concentration of  $[\text{Fe}(\text{CN})_6]^{3-/4-}$  (mM). Here,  $D = 0.76 \times 10^{-5}$ ,  $n = 1$ ,  $\nu = 0.05$ , and  $C = 5.0$ . The

calculated electroactive surface area of Al-MCF/CPE is  $0.107 \text{ cm}^2$ , which is much higher than  $0.078 \text{ cm}^2$  of CPE. Therefore, these results demonstrate that Al-MCF can effectively improve the electroactive area of the electrode surface.

The capability of electron transfer of bare and modified electrodes was investigated by electrochemical impedance spectrometry (EIS), and the results are illustrated in Figure 3B. In the EIS plots of the bare CPE (curve a), a clear semicircular area is observed. However, no obvious semicircular area is noticed in the EIS plot for the Al-MCF/CPE (curve b). Indeed, these results confirm that the Al-MCF can improve the conductivity of modified electrode.

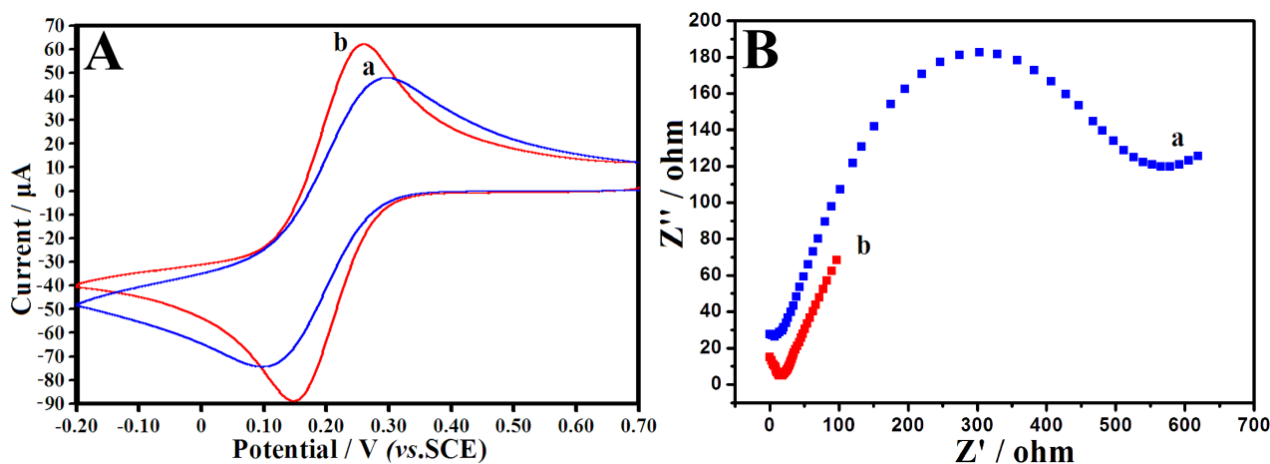


**Figure 3.** Cyclic voltammograms (A) and Nyquist plots (B) of the bare CPE (a) and Al-MCF/CPE (b) in  $5.0 \text{ mM } [\text{Fe}(\text{CN})_6]^{3-/4-}$ .

### 3.3. Electrochemical behavior of Ethyl Parathion

Figure 4 displays the cyclic voltammograms obtained for  $0.30 \text{ mg/L}$  EP at the bare CPE (curve a) and Al-MCF/CPE (curve b) in PBS ( $\text{pH} = 7.0$ ). A very small peak is observed at  $-0.13 \text{ v}$  for the bare CPE, which correspond to the oxidation process of EP. However, a pair of well-defined peaks (peak I at  $-0.10 \text{ v}$ , peak II at  $-0.16 \text{ v}$ ) were noticed for the Al-MCF/CPE, which originates from the redox processes taking place at the surface of this electrode. These results are in well agreement with those previously reported by other research groups [9]. On the basis of these results, a mechanism of the electrochemical reaction of EP at electrodes was attempted, and it is presented in Scheme 1. It is noteworthy that the peak current of EP is more intense when Al-MCF is used as a modifier for CPE. The strong enhancement can be explained by the higher electroactive area, excellent conductivity, and strong adsorptivity of the electrode induced by Al-MCF.

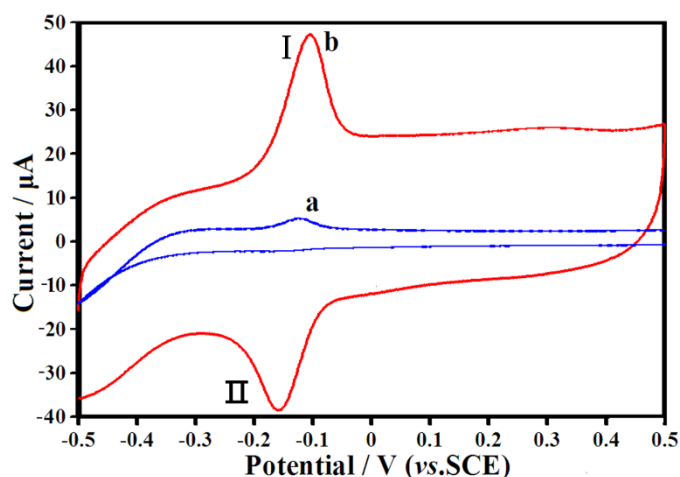
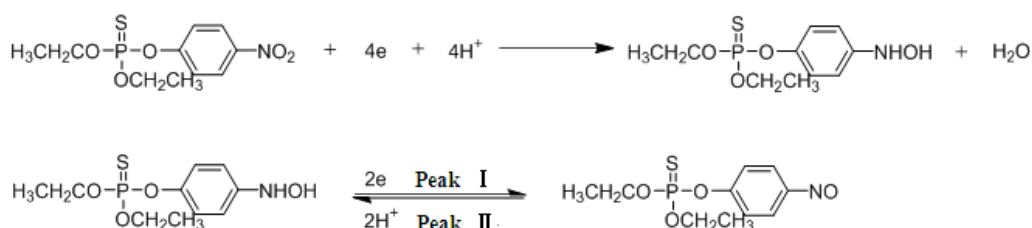


**Figure 4.** Cyclic voltammograms obtained for 0.30 mg/L EP with bare CPE (a) and Al-MCF/CPE (b).



**Scheme 1.** Electrochemical reaction mechanisms of EP

### 3.4. Optimization studies for the measurement of EP at Al-MCF/CPE

Figure 5A shows the effect of the amount of Al-MCF on the current response of EP. As seen, the current response increased with the content of Al-MCF in modified electrode and reached a maximum at 2.44 wt.% Al-MCF. Further increased in Al-MCF content led to a significant decrease in the current response. Al-MCF possess high accumulation efficiency and super signal amplifying power. So, a small amount of Al-MCF will notably enhance the current response of EP. However, large amount of Al-MCF certainly increases the background current which will lead to a decreased of the current response of EP [24]. Thus, 2.44 wt.% was the optimum loading with Al-MCF, and the sample containing this percent of mesoporous silica-alumina was selected for the subsequent step of our research.

Both the peak current and the peak potential ( $E_p$ ) of EP could be influenced by pH of the electrolyte solution. Hence, the effect of pH on the current response and  $E_p$  of EP was investigated in the range of 2.0 - 12.0 (Figure 5B). The peak current increased significantly with the increase of pH in the range of 2.0 - 7.0, and then decreased for higher pH values. Therefore, the optimum value of pH for a functional EP is 7.0. It was also noticed that, as the pH increases, the peak potential shifted to negative values indicating the proton participation in the electrochemical reaction of EP. The equation of the plot  $E_p$  vs pH is  $E_p = 0.2470 - 0.05687 \text{ pH}$  ( $R = 0.999$ ) with a slope value of  $-56.9 \text{ mV/pH}$ , which is close to the theoretical value of  $-59.0 \text{ mV/pH}$ . This finding shows that the number of electrons transferred was

equal to the number protons involved in the electrochemical oxidation of EP, which is in agreement with Scheme 1 describing the reaction taking place at the electrode surface.

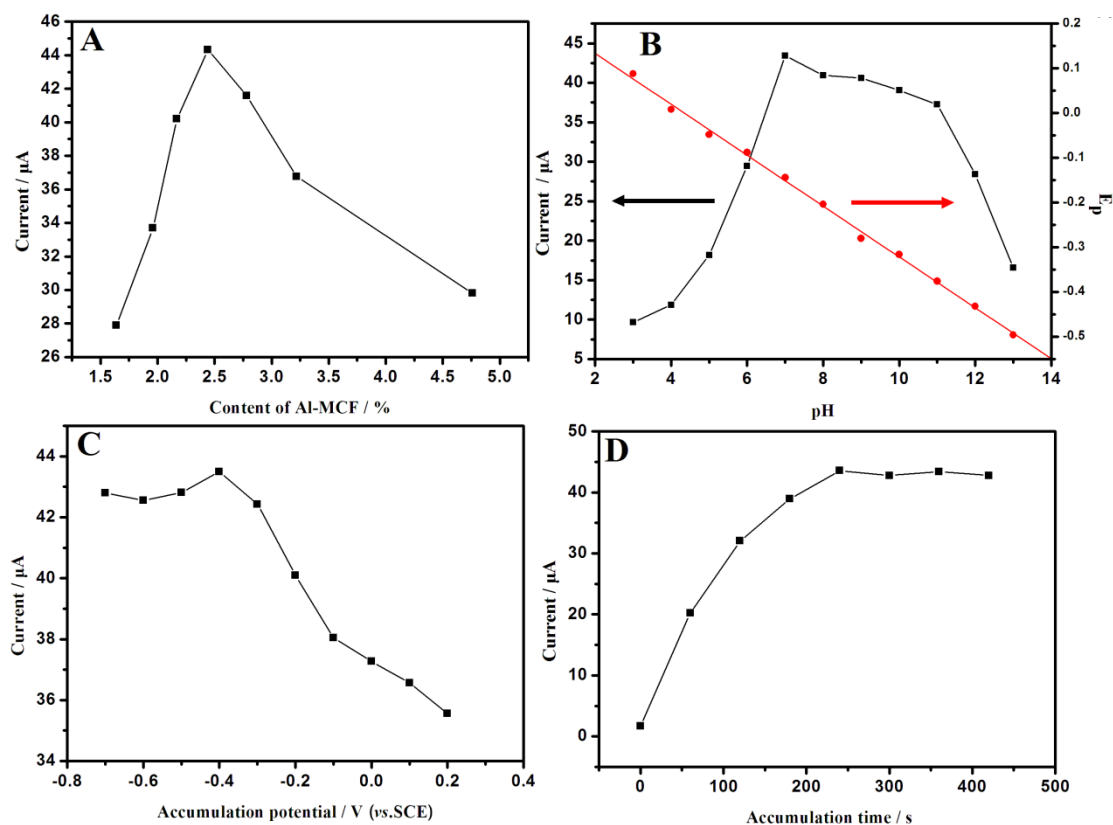


**Figure 5.** The effect of content of Al-MCF (A), accumulation potential (C), and accumulation time (D) on the peak current for 0.30 mg/L EP. The effect of pH on peak current and peak potential for 0.30 mg/L EP (B).

As shown in Scheme 1, in the electrochemical reaction process of EP, at first, the nitro group in EP is reduced to arylhydroxylamine under a negative potential [9], therefore a negative potential should be applied in the accumulation period. The influence of the accumulation potential on the peak current for 0.30 mg/L EP was investigated in the range of  $-0.70$  -  $0.20$  V (Figure 5C). The peak current of EP increased rapidly as the accumulation potential shifted from  $0.20$  to  $-0.40$  V, then it slightly changed when the accumulation potential was lower than  $-0.40$  V. Thus, an accumulation potential of  $-0.40$  V was considered as optimum and selected for the further investigation.

The effect of accumulation time on the peak current for 0.30 mg/L EP is illustrated in Figure 5D. The peak current is found to increase with time up to 240 s, these results suggest that accumulation is efficient to improve the peak current. Accumulation time longer than 240s, the peak current was changed slightly, indicating that the amount of EP on the surface of Al-MCF/CPE tends to a limiting value. Therefore, the optimum accumulation time selected for the measurement was 240 s.

3.5. Calibration curve

Once the optimal experimental conditions were established, the calibration curves were generated for the electrochemical reaction of EP (Figure 6). It can be seen that there is a good linear relationship between EP concentration and current response. The current response increased with EP concentration in the range of 0.010 to 0.10 mg/L and 0.10 to 1.0 mg/L, with a detection limit of 0.0050 mg/L (S/N = 3). The regression equations can be expressed as follows.

$$i_p(\mu\text{A}) = 233.4 C (\text{mg/L}) - 1.355$$

$$i_p(\mu\text{A}) = 66.85 C (\text{mg/L}) + 20.32$$

with the correlation coefficients of 0.999 and 0.990, respectively. The comparison of Al-MCF/CPE with other modified electrodes for the EP determination are listed in Table 1. As can be seen, Al-MCF/CPE shows relatively high sensitivity and wide linearity toward the electrochemical detection of EP.

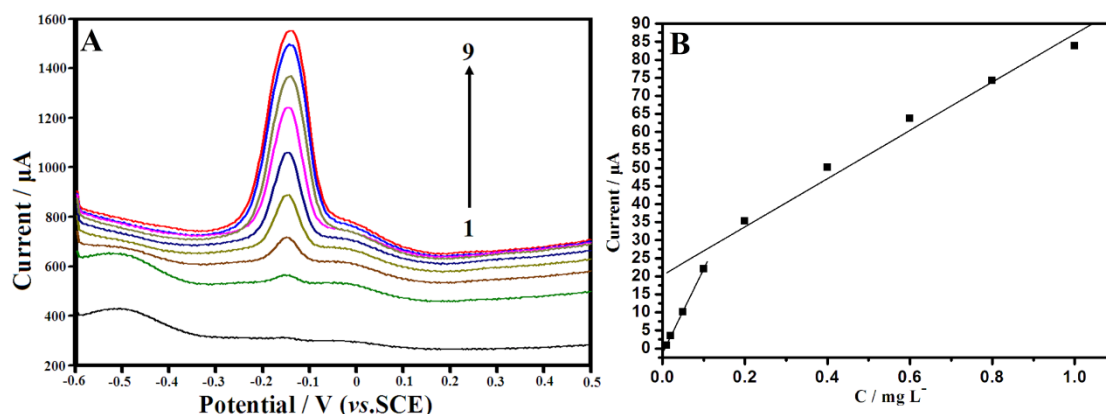


**Figure 6.** SWV curves of EP at the Al-MCF/CPE in pH 7.0 PBS with different concentrations (from 1 to 9: 0.010; 0.020; 0.050; 0.10; 0.20; 0.40; 0.60; 0.80 and 1.0 mg/L, respectively) (A) and linear relationship between the current response and the EP concentration (B).

**Table 1.** Comparison of the Al-MCF/CPE with other modified electrodes for the EP determination

Modified electrode	Linear range (mg/L)	Detection limit (mg/L)	Reference
Molecularly imprinted nano-TiO <sub>2</sub> self-assembled film electrode	0.015 – 2.9	0.0029	8
Molecularly imprinted polymer modified CPE	0.00050 – 0.26	0.00015	9
Molecularly imprinted polyethyleneimine/silica gel films modified electrode	0.015 – 15	0.0030	10
Carbon nanoparticles and halloysite nanoclay modified CPE	0.00035 – 1.4	0.00011	11
Zirconiumoxide-laponite nanocomposites-modified glassy carbon electrode	0 – 58	1.6	12
Silver nanoparticle-modified electrode	0.012 – 2.3	0.012	13
Al-MCF/CPE	0.010 – 0.10, 0.10 – 1.0	0.0050	This work

The reproducibility and stability of the sensor were evaluated using a 0.30 mg/L EP solution. Six independently-prepared Al-MCF/CPEs were investigated in the current of EP. The relative standard deviation (RSD) was 6.2%. For 11 successive measurements of one Al-MCF/CPE, the RSD was 2.9%. The stability of the Al-MCF/CPE was investigated after long-term storage in air for one week, and it was observed that 97% of the original peak current was retained.

The influence of potential interferences for the detection of 0.30 mg/L EP was investigated by SWV using the above-optimized conditions. In this work, the tolerance limit was defined as the molar ratio of interference/SY that caused a  $\pm 5.0\%$  change in the current response of EP. It was found that 1000-fold glucose and sucrose, 500-fold  $\text{Na}^+$ ,  $\text{K}^+$ ,  $\text{Ca}^{2+}$ ,  $\text{Mg}^{2+}$ ,  $\text{Cu}^{2+}$ ,  $\text{Zn}^{2+}$ , and  $\text{Fe}^{3+}$ ; as well as 100-fold vitamin B<sub>1</sub>, B<sub>2</sub>, C, and E did not interfere with the determination of EP. However, methyl parathion severely interfered with the determination of EP, because of their similar molecular structure. In the light of these encouraging results, it can be stated that the prepared sensor is suitable for quantitative detection of the total amount of parathion.

### 3.6. Electrochemical detection of EP in cabbage samples

To evaluate the feasibility of the developed method, the Al-MCF/CPE was employed for the determination of EP in cabbage sample by using a standard addition method. The results are summarized in Table 1. The recoveries were in the range of 94.4 – 110 %. The resulted values suggest that the described method can be used for the accurate detection of EP in real samples.

**Table 2.** Determination of EP in cabbage sample

Original ( $\mu\text{g/g}$ )	Added ( $\mu\text{g/g}$ )	Found ( $\mu\text{g/g}$ )	Recovery (%)
0.00	2.50	2.36	94.4
0.00	5.00	54.9	110
0.00	10.0	9.62	96.2

## 4. CONCLUSION

Al-doped mesoporous cellular foam silicas were synthesized and used to prepare an EP electrochemical sensor. The results showed that the Al species were uniformly distributed within the Al-MCF framework, which proved to be important sites for maintaining three-dimensional mesoporous organization of Al-MCF. The Al-MCF/CPE sensor exhibited excellent electrochemical properties. It was also showed that it displays outstanding performance for the electroanalysis of EP when compared with bare CPE. It is worth emphasizing that the proposed electrochemical sensor is ease to prepare while the excellent results obtained for the detection of EP recommend it as a promising tool for the fast and accurate identification of the parathion in real samples.

## ACKNOWLEDGEMENTS

This article was supported by the Guangxi Science and Technology Major Projects (NO. AA17204043-2), the Natural Science Foundation of Guangxi for Youth (No. 2015GXNSFBFA139037), the Guangxi Funds for Special-invited Experts and the Guangxi Academy of Agricultural Sciences Funds for Distinguished Young Scholars (2018YM26).

## References

1. L. Roldan-Tapia, F.A. Nieto-Escamez, E.M. del Aguila, F. Laynez, T. Parron and F. Sanchez-Santed, *Neurotoxico. Teratol.*, 28 (2006) 694.
2. T.J. Yang and M.R. Lee, *Talanta* 82 (2010) 766.
3. X. Zheng, L. He, Y. Duan, X. Jiang, G. Xiang, W. Zhao and S. Zhang, *J. Chromatogr. A*, 1358 (2014) 39.
4. M.T. Jafari, M. Saraji and M. Mossaddegh, *J. Chromatogr. A*, 1466 (2016) 50.
5. R. Bala, R.K. Sharma and N. Wangoo, *Sensors Actuators B*, 210 (2015) 425.
6. J. Wang, M.P. Chatrathi, A. Mulchandani and W. Chen, *Anal. Chem.*, 73 (2001) 1804.
7. X. Hua, L. Wang, G. Li, Q. Fang, M. Wang and F. Liu, *Anal. Methods*, 5 (2013) 1556.
8. C. Li, C. Wang, C. Wang and S. Hu, *Sensors Actuators B*, 117 (2006) 166.
9. T. Alizadeh, *Electroanalysis*, 21 (2009) 1490.
10. Q. Yang, Q. Sun, T. Zhou, G. Shi and L. Jin, *J. Agric. Food Chem.*, 57 (2009) 6558.
11. B.J. Sanghavi, G. Hirsch, S.P. Karna and A.K. Srivastava, *Anal. Chim. Acta*, 735 (2012) 37.
12. M.P.N. Bui and S.S. Seo, *J. Appl. Electrochem.*, 45 (2015) 365.
13. C.A. de Lima, E.R. Santana, J.V. Piovesan and A. Spinelli, *Anal. Bioanal. Chem.*, 408 (2016) 2595.
14. Z. Xue, X. Hu, H. Rao, X. Wang, X. Zhou, X. Liu and X. Lu, *Anal Methods*, 7 (2015) 1167.
15. M.K. Bojdi, M. Behbahani, F. Omidi and G. Hesam, *New J. Chem.*, 40 (2016) 4519.
16. L. Xie, Y. Ya and L. Wei, *Int. J. Electrochem. Sci.*, 12 (2017) 9714.
17. Y. Ya, C. Jiang, F. Yan, L. Xie, T. Li, Y. Wang and L. Wei *J. Electroanal. Chem.*, 808 (2018) 107.
18. L. Wei, Y. Zhao, Y. Zhang, C. Liu, J. Hong, H. Xiong and J. Li, *J. Catal.*, 340 (2016) 205.
19. J. Li, L. Zhou, X. Han, J. Hu, H. Liu and J. Xu, *Sensors Actuators B*, 138 (2009) 545.
20. N.A. Jamalluddin and A.Z. Abdullah, *J. Mol. Catal. A:Chem.*, 414 (2016) 94.
21. S. Chen, J. Li, Y. Zhang, Y. Zhao, K. Liew and J. Hong, *Catal. Sci. Technol.*, 4 (2014) 1005.
22. M.G. Colmenares, U. Simon, F. Schmidt, S. Dey, J. Schmidt, A. Thomas and A. Gurlo, *Micropor. Mesopor. Mat.*, 267 (2018) 142.
23. A.J. Bard and L.R. Faulkner, *Electrochemical Methods: Fundamentals and Applications*, second ed., Wiley, (1980) New York, USA.
24. H. Lin, T. Gan and K. Wu, *Food Chem.*, 113 (2009) 701.